C_xF_y Polymer Film Deposition in rf and dc C_7F_{16} Vapor Plasmas

Y. Sakai, M. Akazawa, Yosuke Sakai, H. Sugawara and M. Tabata
Graduate School of Engineering, Hokkaido University, Sapporo 060-8628, Japan

C. P. Lungu and A. M. Lungu
National Institute of Lasers, Plasma and Radiation Physics, PO Box MG-37, Bucharest, Romania

C_xF_y polymer film was deposited in rf and dc Fluorinert vapor (C_7F_{16}) plasmas. In the plasma phase, the spatial distribution of optical emission spectra and the temporal concentration of decomposed species were monitored, and kinetics of the C_7F_{16} decomposition process was discussed. Deposition of C_xF_y film has been tried on substrates of stainless steel, glass, molybdenum and silicon wafers at room temperature in the vapor pressures of 40 and 100 Pa. The films deposited in the rf plasma showed excellent electrical properties as an insulator for multi-layered interconnection of deep-submicron LSI, i.e. the low dielectric constant ~2.0, the dielectric strength ~2 MV/cm and the high deposition rate ~100nm/min at 100W input power.

Keywords : Fluorocarbon plasma, low dielectric constant film, precursor, plasma-enhanced chemical vapor deposition, material characterization.

1. INTRODUCTION

The chip area of logic large-scale integrated circuits (LSIs) is occupied by a large amount of interconnection space. The long inter-modular connection provides nontrivial parasitic capacitance and resistance that cause signal propagation delay.

In deep-submicron LSIs, this problem will become severer. To reduce the signal propagation delay, it is important to minimize the parasitic capacitance and resistance of the interconnection wires. Actually the parasitic resistance was reduced by copper interconnection wires instead of conventional aluminum[1].

Reduction of the parasitic capacitance has been attempted using plasma enhanced chemical vapor deposition (PECVD) of amorphous fluorinated carbon films, CH_4/CF_4 [2], CF_4, C_2F_6 [3], C_4F_8 [4], CFC-113/C_2H_4 [5] and $O_2/FSi(OC_2H_5)_3$ [6]. They provided successful formation of films with dielectric constants between 2.1 and 2.8. These films showed good adhesion to silicone substrates and good thermal stability by reducing the F/C ratio of source materials [4], and using material with low bulk dielectric constant [7]. Among these studies, CF_2 precursor was found to play an essential role in the fluorocarbon film formation [8]. In the authors laboratory, the dielectric films deposited in rf plasma of fluorocarbon $(C_3F_7)_3N/(C_4F_9)_3N$ and $C_8F_{18}/C_8F_{16}O$ vapor have revealed excellent dielectric properties for deep-submicron LSIs [9,10].

In this paper we present a film deposited using a novel fluorocarbon source material of C_7F_{16}, and its decomposition species and process in plasma. C_7F_{16} is a liquid at room temperature and has a low F/C ratio, a low dielectric constant of 1.81, and a low refractive index of 1.261. Fluorocarbon liquids are fluorinated compounds that in recent years have been used as solvents for cleaning purposes. They are not regulated using due to depletion of the terrestrial ozone layer and are nonflammable and highly resistant to thermal breakdown.

2. EXPERIMENTAL APPARATUS AND METHOD

Figure 1 shows a schematic diagram of the experiment. A discharge chamber is made of a stainless steel cylinder of 300 mm in diameter and 420 mm in height. Electrodes in the chamber are made of stainless steel plates of 100 mm in diameter. After the chamber was evacuated up to 10^{-4} Pa by a mechanical rotary and diffusion pumps, C_7F_{16} monomer vapor, which is stored

as liquid phase in a 200 ml glass vessel attached to the plasma reactor, is introduced. The pressure of C_7F_{16} vapor is kept 40 or 100 Pa by adjusting the flow rate of the vapor.

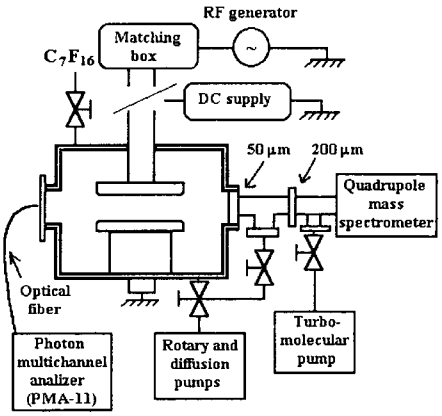

Fig. 1. A schematic diagram of the experimental set-up.

The power into the plasma was supplied by a regulated high voltage dc generator or a 13.56 MHz rf generator(RFPP Inc., RF-5S type). The dc current was fixed at 10 mA, and the rf power was fixed at 100 W.

A quadrupole mass spectrum analyzer (QMS; Shimazu Co.Ltd. type) is connected through a cylinder pumped down($\sim$10 Pa) separately to this reactor. With this differential pumping system, the pressure in the mass spectrometer was kept $\sim 10^{-4}$ Pa. The emission spectra from the plasma was observed by a Photonic Multichannel Spectral Analyzer (resolution;1.5nm) through a quartz lens and optical fiber.

The film is deposited on substrates; stainless steel, glass, molybdenum and silicon wafers at room temperature. The thickness of the films is measured by ellipsometry and stylus methods.

The dielectric constant of the film is determined by measuring the capacitance-voltage (C-V) characteristics on an Au/fluoropolymer/n+-Si(100) structure diode at 100 kHz.

3. RESULTS AND DISCUSSION

3.1. In plasma phase

(a) Mass analysis of decomposed species

Figures 2 shows the temporal evolution of decomposed species of C_7F_{16} in a dc discharge plasma. Here, the C_7F_{16} vapor is sealed in the chamber at 100Pa. Discharge current is 10mA. This figure indicates that C_7F_{16} is decomposed mostly into C, F, CF, CF_2, CF_3, C_2F_3, C_3F_4, C_2F_5, C_3F_3 and C_3F_5. The relative concentration of the heaviest species always decreases, because of the decomposition.

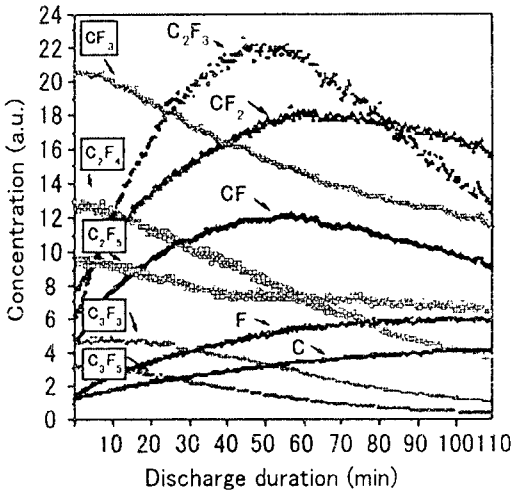

Fig. 2. Temporal evolution of the decomposed species observed using a QMS in a dc plasma. C_7F_{16} vapor is sealed by a pressure of 100Pa. A plasma current; 10 mA, and a voltage; 500 V.

The relative concentration of CF, CF_2 and C_2F_3 species first increases, because of a decomposition process of C_7F_{16}. However, after about 60 minutes from the plasma ignition the CF, CF_2 and C_2F_3 concentrations decrease, due to deposition as polymer film on the electrodes and on the wall of the reaction chamber.

(b) Emission spectra

Figure 3 shows a typical spatial distribution of the emission spectra obtained in (a) rf and (b) dc discharges, along the axis of the electrode with a spatial resolution of 1 mm.

In the rf plasma case, the plasma is almost uniform except near the grounded electrode. In particular, the intensity from CF_2 radical identified by the emission band at 321nm and from C_2 species identified from the Swan band at 468.5nm are shown in the medallion of figure 3 (a). The former values are from 2 to 3 times larger than the latter value. The maximum appears in the bulk, but a little bit biased to the grounded electrode.

In the dc case, a glow plasma is a classical configuration with a column in the bulk and sheathes near the anode and the cathode. The intensities from CF_2 and C_2 are plotted in the medallion of figure 3 (b). In the anode region, the intensity from C_2 is larger than the intensity from CF_2 radical owing to the preferential excitation of C_2. On the other hand, near the cathode the intensity from CF_2 radical is larger than the C_2 value. In the dc case the structure is more prominent.

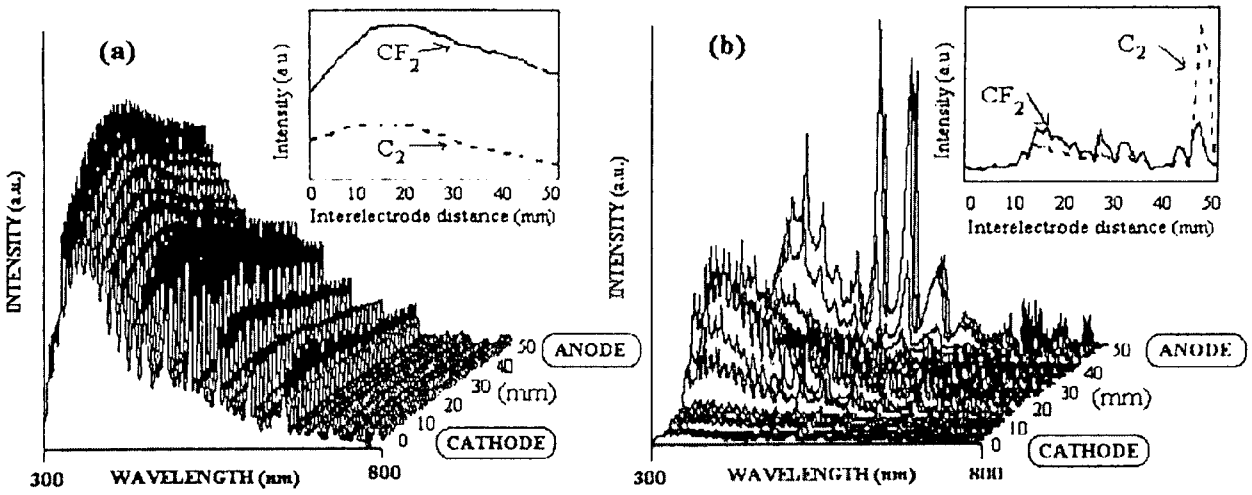

Fig. 3. Spatial distribution of optical emission spectra in C_7F_{16} vapor of 100Pa (a) rf plasma of 100W, and (b) dc discharge of 10 mA, 500 V. In medallions are plotted the intensities of CF_2 and C_2 species.

Through the optical emission spectra, the CF_2 formation in the plasma is confirmed. The strong characteristics of CF_2 (A1B1 - X1A1) bands are seen at 245.76 nm, 248.78 nm, 251.86 nm, 255.06 nm, 249.50 nm, 152.85 nm, 265.24 nm, 267.55 nm, 271.13nm and, 279.98 nm. The formation of CF_2 precursor was confirmed also in a qaudruploe mass spectrometry measurement of figure 2.

(c) Kinetics of C7F16 decomposition

CF and CF_2 radicals were already reported as precursors of CFx film formation [11, 12]. Figure 2 indicates the presence of C_2F_3 radical with the same behavior as CF and CF_2 precursor. C_2F_3 radical is identified as one of the precursors of C_xF_y films in this work. We may expect the following decomposition processes based on the above results and literature [13,14]:

C_7F_{16}	→	$C_2F_5 + 2C_2F_4 + CF_3$	(1)
C_7F_{16}	→	$2CF_3 + C_3F_5 + C_2F_4 + F$	(2)
C_7F_{16}	→	$2C_2F_5 + 3CF_2$	(3)
C_2F_5	→	$CF_2 + CF + 2F$	(4)
C_3F_5	→	$C_2F_3 + CF_2$	(5)
C_3F_3	→	$C_2F_3 + C$	(6)
C_2F_3	→	$CF_2 + CF$	(7)
C_2F_4	→	$CF_3 + CF$	(8)

3.2 Film characterization

For film characterization we took the film only deposited in rf discharges, since it was defect free structure and better quality, while the film deposited in dc plasma was too worse to characterize. The films deposited on Si substration were analyzed after deposition of thickness between 0.6 and 5 ㎛.

(a) XPX analysis

The excitation source of the present XPS is Mg K α radiation source (h v =1253.6 eV). The obtained survey spectrum is shown in Figure 4. The strong peak of the F vapor of 100Pa (a) rf plasma of 100W, and (b) dc.1s level indicates successful formation of the fluoropolymer films. The F/C ratio estimated from the intensity of the C 1s and F 1s core levels considering the relative sensitivity factor (RSF), is higher than 1.6. This result indicates that large amount of fluorine is contained in the film.

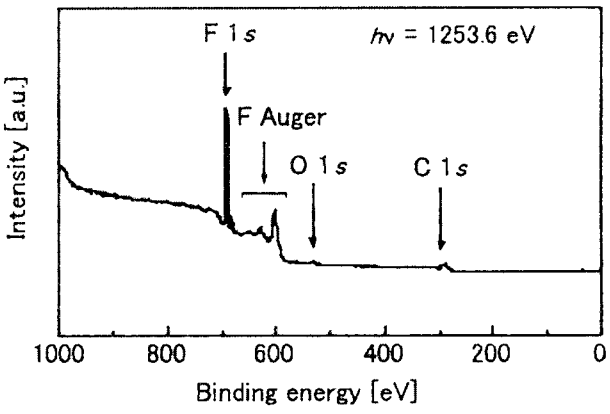

Fig. 4. XPS survey spectrum for the film deposited in rf C_7F_{16} vapor plasma.

The C 1s core level spectra of the film formed in C_7F_{16} vapor at 60Pa for various deposition times show significant chemical shift as shown in figure 5, which is unique to a fluorinaed carbon film. In a deposition time of 10 sec the CF_2 peak is especially emphasized. With increasing the time, the CF and C-CF_x peaks become prominent. After 30 sec deposition, the film thickness becomes around 90nm.

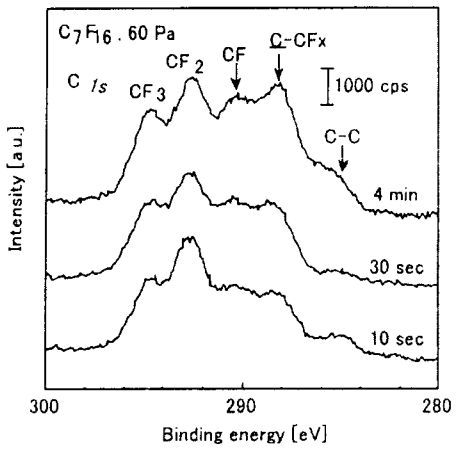

Fig. 5. The *C1s* core level spectra in XPS for the film deposited in rf C_7F_{16} vapor plasma of 60Pa.

However, by this thickness the electrical and optical properties are poor in reproducibility. With increasing the time up to a thickness of 1 ㎛, the properties become excellent as given in Table 1 and reproducible.

According to Cunge and Booth[11], the key species for film polymerization in fluorocarbon discharges are CF_2 radical and atomic fluorine. The present result indicates also that C_2 plays an important role in film formation. When the CF_2 concentration in plasmas increases, the deposition rate of films increases. The polymer structure is also affected by the ratio of the CF_2 to C_2 concentration. C_2F_3 radical is present and may be a precursor to the film formation as well as CF and CF_2[11].

(b) FTIR study

The FTIR result of the films is shown in figure 6. It is shown that the film has CF_2 sequences with CF_3 groups at the end of the chain sequence.

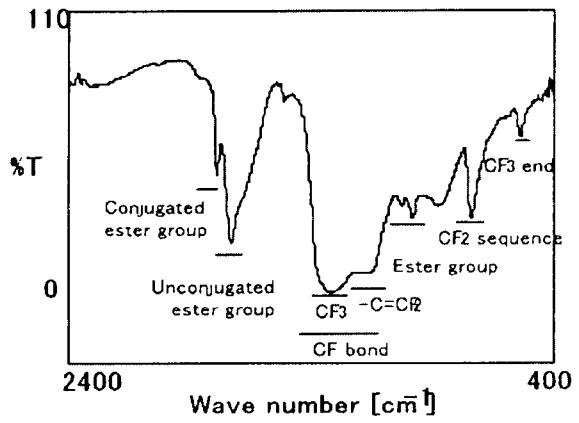

Fig. 6. FTIR spectrum of the film.

The absorption spectrum in the region of 1790 and 1700 cm^{-1} suggests the formation of unconjugated and/or conjugated ester groups. This film shows strong absorption in the regions 1820~1620 cm^{-1}, and 1380~1000 cm^{-1}, where the absorption by C-F, $-CF_2-$, $-CF_3$, $-C=CF_2$, and $-CF=CF_3$ is overlapped [15]. This result shows the content of large amount of fluorocarbons and formation of long chains $-(CF_2)n-$ incorporated in the film. The absorption seen in the region of 1250~1150cm^{-1} may be resulted from the contents of amines (C-N) [15]. Those of 1780cm^{-1}, 1710cm^{-1}, and 1150~1030cm^{-1} may be assigned by ester groups (C=O) [15].

(c) Deposition rate, refractive index, dielectric constant and dielectric strength

Using an ellipsometer the thickness and refractive index were studied. The obtained refractive index was 1.38 ±0.01. Such low refractive index is peculiar to the fluoropolymers.

The refractive index of amorphous perfluoro-polymers composed by only C-C, C-F and C-O bonds without C=O and C=C bonds range are from 1.31 to 1.35 [16]. Considering the results of XPS and FTIR, the present slightly higher value of the refractive index may indicate the content of $-CF=CF_2$, and $-C=CF_2$ bonds resulting in the cross-linking structure.

The capacity was measured by making a Au/CF polymer/n^+Si(100) diode structure with Mg/Al ohmic contact on the backside. After the deposition, the Au electrodes were formed by the vacuum evaporation onto the as-deposited polymer films. The capacity was measured at a frequency of 100 kHz. The refractive index n at the high frequency is related with ε_r through Maxwell's equation as, $\varepsilon_r = n^2$.

The dielectric strength was obtained by plotting the I-V characteristics for a sample having a Au/CF polymer/molybdenum structure with the electrode area of 0.04 cm^2. The applied voltage was increased up to the breakdown voltage by 10 V step. The minimum value of the breakdown field was given to be 2MV/cm.

The deposition rate, refractive index n, dielectric constant ε_r and dielectric strength Es for all the samples are summarized in Table 1 along with the data from references [2, 4, 6]. It was shown that, for the present film, the deposition rate and the breakdown strength were higher, and the dielectric constant and the refractive index were smaller than the values of films obtained using other source materials.

3.3 Discussion of film structure

The ESR spectrum shown in figure 7 observed at room temperature indicates the presence of the following secondary carbon radical:

$$\sim CF_2 - CF - CF_2 \sim$$

Table 1. The film properties for different source materials. The deposition rate for C_7F_{16} given at 60 Pa. n and ε_r indicate the refractive index and dielectric constant, respectively.

source material	Power [W]	Deposition rate [nm/min]	n	ε_r	Dielectric strength [MV/cm]
C_7F_{16} [pres. work]	100 rf	110 (60)	1.38	2.0	> 2.4
CH_4 [ref.2]	200	7-19	-	2.6 - 4.5	-
CH_4 + CF_4 [ref. 2]	200	10	-	2.1 - 4.0	> 1
C_4F_8 [ref.4]	300	-	1.42 - 1.43	2.2 - 2.5	-
O_2, SiF_4, Ar O_2, Fsi $(OC_2H_5)_3$ [ref.6]	1000 helicon	-	-	2.8 - 3.2	-

The net increase in the CF_2 density indicates the production processes of a large amount of precursors for polymer film formation. Analyzing the FTIR spectra, the film has long CF_2 sequences bearing CF_3 groups at the end of the chain sequence.

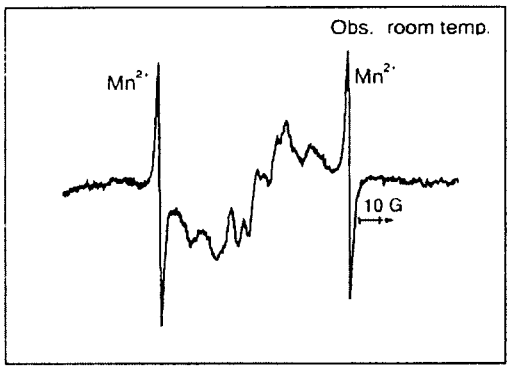

Fig. 7. ESR spectrum.

This peak can be assigned to that of the fluorinated vinyl groups, i.e. -C=CF_2, and/or also long CF_2 chains which are incorporated in this material $(CF_2)_n$ [17]. The formation of ester groups was observed by FTIR and XPS analyses, and was supposed by presence of the oxygen as the air absorbed in the precursor fluid. The increasing temperature of the active species in the rf discharge may be a reason for the ester formation.

4. CONCLUSION

In dc and rf discharge plasmas, C_7F_{16} molecule was shown to be decomposed into C, F, CF, CF_2, CF_3, C_2F_3, C_2F_4, C_2F_5, C_3F_4 and C_3F_5. In rf discharges the emission spectra showed that the excited species CF_2 and C_2 were distributed uniformly along the axis between electrodes, whereas in dc discharge C_2 species was concentrated in the anode region and CF_2 species was found near cathode region.

In the rf discharges, it was found that the fluorinated vinyl groups, i.e. -C = CF_2, or long CF_2 chains was incorporated in the material. The film was obtained with a deposition rate of 170 nm/min, a low dielectric constant (ε_r=2) and breakdown strength larger than 2MV/cm.

ACKNOWLEDGMENTS

Authors are grateful to Mr. Soon-Youl for kind helping edition of this paper.

REFERENCES

[1] N. Rohrer et.al: Proc. ISSCC 1998, FP 15.6 (1998).
[2] K. Endo and T. Tasumi: J. Appl. Phys. 78 (1995) 1370.
[3] K. Endo and T. Tasumi: Appl. Phys. Lett. 68 (1996) 2864.
[4] K. Endo and T. Tasumi: Jpn. J. Appl. Phys 36 (1997) L1531.
[5]O. Tsuji, T. Minagichi, H. Nakano and T. Tatsuta: Jpn. J. Appl. Phys. 36 (1997) 4964.
[6]S. M. Yun, H.Y. Chang, K. S. Oh and C.K. Choi: Jpn. J. Appl. Phys. 38 (1999) 4531.
[7] T. C. Nason, J. A. More and T. M. Lu: Appl. Phys. Lett. 60 (1992) 1866.
[8]K. Takahashi, M. Hori, M. Inayoshi and T. Goto: Jpn. J. Appl. Phys. 35 (1996) 3635.
[9]C.P. Lungu, A.M.Lungu, M.Akazawa, Y.Sakai, H.Sugawara and M. Tabata, Jpn. J. Appl. Phys. Vol.38 No.12B (1999) L1544 - L1546
[10] C.P.Lungu, A.M.Lungu, Y.Sakai, H.Sugawara, M.Tabata, M.Akazawa and M.Miyamoto, Vacuum (2000) accepted

[11] Cunge C, and Booth J. P., J. Appl. Phys., 1999; 85: p3952-3959.
[12] Oda T., Takahashi T., Nahano H., Masuda S., IEEE Trans. Ind. Applicat., 1993; 29: p787-792.
[13] Penetrante B. M., Norman J., Hsiao M. C., Jpn. J. Appl. Phys., 1997; 36; 7B: p5007-5017.
[14] Suzuki C., Sasaki K., Kadota K., Jpn. J. Appl. Phys., 1998; 37: p5763-5766.
[15]R. M. Silverstein, F. X. Webster: Spectrometric Identification of Organic Compounds, 6-th ed. (New York: Wiley 1997) Chapter 3.
[16] M. Fuji, K. Sakurai, and A. Fujita, KIKAN KAGAKU SOUSETSU, 39 (1998) 122.
[17] Tabata M., Sadahiro Y., Sone T., Yokota K., Ishikawa Y., J. Polym. Sci. 1998; 36; A: p2457-2461.